Coupled Kinetics of ATP and Peptide Hydrolysis by *Escherichia coli* FtsH Protease

Robert C. Bruckner,*[,‡] Paul L. Gunyuzlu,[§,||] and Ross L. Stein[‡,⊥]

Departments of Chemical Enzymology and Biotechnology, Pharmaceutical Research Institute, Bristol-Myers Squibb Company, P.O. Box 80400, Wilmington, Delaware 19880

Received April 2, 2003; Revised Manuscript Received July 16, 2003

ABSTRACT: FtsH from *Escherichia coli* is an ATP- and Zn^{2+}-dependent integral membrane protease that is involved in the degradation of regulatory proteins such as σ^{32} and uncomplexed subunits of membrane protein complexes such as secY of the protein translocase. We describe a protocol for solubilizing the recombinant enzyme from inclusion bodies and its subsequent refolding and purification to near homogeneity. This is a high-yield protocol and produces in excess of 20 mg of purified FtsH per liter of *E. coli* culture. We found that refolded FtsH has biochemical properties similar to detergent extracted overexpressed protein described previously. FtsH forms a large complex with an apparent mass of 1200 kDa as determined by gel filtration. Both ATPase and protease activities are coincident with this large complex; smaller forms of FtsH do not exhibit either activity. While FtsH-catalyzed hydrolysis of ATP can occur in the absence of protein substrate ($k_c = 22$ min^{-1}; $K_m = 23$ μM), proteolysis shows an absolute dependence on nucleoside-5′-triphosphates, including ATP, CTP, and various analogues. In the presence of 5 mM ATP, FtsH catalyzes the hydrolysis of σ^{32} with the following observed kinetic parameters: $k_c = 0.18$ min^{-1} and $K_m = 8.5$ μM. Significantly, this reaction is processive and generates no intermediate species, but rather, approximately 10 peptide products, all of MW <3 kDa. FtsH protease also efficiently hydrolyzes the peptide Phe-Gly-His-^{NO_2}Phe-Phe-Ala-Phe-OMe. Hydrolysis occurs exclusively at the ^{NO_2}Phe−Phe bond ($k_c = 2.1$ min^{-1}; $K_m = 12$ μM), and like proteolysis, shows an absolute dependence on NTPs. We propose a mechanism for the coupled hydrolytic activities of FtsH toward ATP and peptide substrates that is consistent with a recently proposed structural model for FtsH.

The *ftsH* gene of *Escherichia coli* encodes an essential ATP- and Zn^{2+}-dependent metalloprotease that resides as an integral component of the inner leaflet of the cytoplasmic membrane of *E. coli* and a wide range of bacterial species (*1*−*7*). While the specificity of FtsH toward protein substrates remains to be fully defined, it is clear that the protease recognizes only a small set of proteins. These include soluble regulatory proteins, such as heat shock sigma factor σ^{32} (*8*), phage λ CII transcriptional activator protein (*9*), and unpaired subunits of membrane protein complexes, such as the secY subunit of the protein translocase (*10*, *11*) and the *a* subunit of the F_1F_0 ATPase (*12*). FtsH has effects on a wide range of bacterial cellular functions. There is evidence that FtsH has a chaperone activity, separate from its ATP-dependent protease activity (*13*). Depletion of FtsH enhances the translocation of protein segments that are normally anchored and retards that of normally translocated proteins (*14*, *15*). For example, FtsH depletion results in the inhibition of the transport of plasmid-expressed β-lactamase into the periplasmic space and its processing to mature form. If β-lactamase is retained in the cytoplasm, β-lactam-based antibiotics will not be degraded (*16*, *17*). An allele of FtsH, mrsC, has been isolated and shown to be required for both the normal decay of mRNA and RNA synthesis (*18*, *19*). Finally, FtsH affects lipid metabolism by regulating levels of UDP-3-*O*-(*R*-3-hydroxymyristoyl)-*N*-acetylglucosamine deacetylase (*4*). These effects on a multitude of activities place FtsH at a biological crossroads. Inhibition of FtsH activity will have far-reaching effects on cellular metabolism, thus making FtsH an ideal target for antimicrobial drug discovery.

At the N-terminus of FtsH are two transmembrane domains that are separated by a 71 amino acid loop that projects into the periplasmic space (*20*) and anchors the protein in the membrane (Scheme 1a,b). The N-terminus is also involved in homo-oligimerization (*21*, *22*) and the association of FtsH with the HflK−HflC complex (*23*). HflKC and FtsH associate through their periplasmic domains; this association regulates FtsH protease activity. Adjacent to the membrane on the cytoplasmic side is a sequence of approximately 220 amino acids containing the Walker A and B, ATP-binding consensus sequences (*24*), followed by a region designated SRH (second region of homology). These motifs are characteristic of the AAA (ATPases associated with different cellular activities) family of proteins. AAA proteins are involved in a number of cellular activities including protein degradation, DNA replication, cell-cycle regulation, organelle biogenesis, and vesicle-mediated protein transport (*25*, *26*). Zinc-metalloproteases contain the characteristic sequence HEXXH where X indicates any uncharged amino acid

* To whom correspondence should be addressed. Telephone: (610) 489-0302. E-mail address: rcbruckner@comcast.net.

‡ Department of Chemical Enzymology.

§ Department of Biotechnology.

|| Present address: Department of Molecular Sciences, AstraZeneca Pharmaceuticals, 1800 Concord Pike, Wilmington, DE 19850.

⊥ Present address: Laboratory for Drug Discovery in Neurodegeneration, Harvard Center for Neurodegeneration and Repair, 65 Landsdowne St., Fourth Floor, Cambridge, MA 02139.

10.1021/bi034516h CCC: $25.00
Published on Web 08/19/2003

Scheme 1[a]

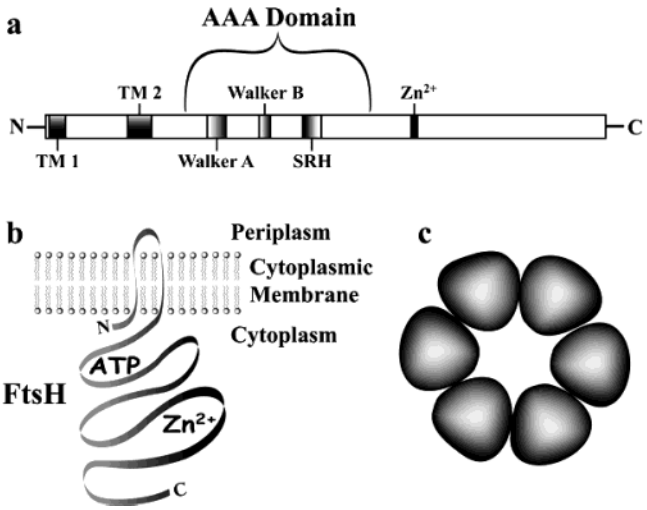

[a] (a) Gene structure of *ftsH*. Protein domains are indicated. (b) Arrangement of FtsH monomer in membrane with ATPase domain and Zn^{2+} binding consensus sequence indicated. (c) Diagram of proposed hexameric quaternary structure.

residue (*27*). Such a consensus sequence (HEAGH) is found toward the C-terminus of FtsH.

A number of AAA proteins have been found to form ring structures, usually hexamers, although heptamers have been observed as well (*26*). The crystal structure of the hexamerization domain (NSF-D2) of the AAA protein *N*-ethylmaleimide-sensitive fusion protein (NSF) has been determined (*28*).

There is evidence that FtsH forms a multimeric complex. FtsH has been reported to migrate as a large complex during gel filtration (*22*), and ring-shaped structures have been observed by electron microscopy (*29*). A model of the FtsH structure has recently been proposed (Scheme 1c) based on the crystal structure of NSF-D2 (*30*). In this model, FtsH forms a hexameric torus. The ATPase domains project into the center of the ring and flex open and closed like an iris upon ATP hydrolysis. The proposed role of ATP hydrolysis is to supply chemical energy that can be transduced into mechanical energy to trigger a conformational isomerization of the enzyme and/or to unwind and translocate the substrate through the hollow core of the complex to the protease active sites.

Expression of membrane-bound proteins is often problematic since high expression levels can disrupt membrane integrity. Overexpression of FtsH has been found to be deleterious to cell growth (*1*). Previous workers had expressed FtsH from a relatively low-level expression vector (*2*). Investigators have reported that high-level expression of FtsH in *E. coli* produces a protein that is resistant to detergent solubilization, an indication that the protein has formed inclusion bodies (*31*). As an alternative approach, we now wish to report the successful solubilization and refolding of FtsH inclusion bodies with an ionic detergent (*N*-laurylsarcosine) (*32*, *33*) in the presence of ATP. The protocol that we report results in a protein preparation with ATP-dependent proteolytic activity against the protein substrate σ^{32}. We went on to purify refolded FtsH and to show that it has properties similar to a detergent-extracted, overexpressed enzyme described by Tomoyasu et al. (*8*). This material was used to undertake a study of this enzyme's coupled mechanism for the hydrolysis of ATP and a peptide substrate.

EXPERIMENTAL PROCEDURES

Materials. Nucleoside-5′-triphosphates, Q-Sepharose Fast-Flow, and a prepacked 25 mL Superose 6 column were obtained from Amersham-Pharmacia. Detergents NP-40, Brij 35, and protease inhibitor cocktail 2 were obtained from CalBiochem. Bacterial protein extraction reagent (BPER)[1] was obtained from Pierce. Hydroxyapatite CHT-2, Econo-Pac Heparin cartridges, protein assay reagent, and Dc Protein assay reagent were obtained from BioRad. Ultrafiltration protein concentrators were obtained from Amicon and Millipore. Preformed SDS−polyacrylamide gels (4−20% gradient), Tris-glycine running buffer, and 2× Tris-glycine sample buffer were obtained from Novex. Ammonium sulfate, Hepes, lysozyme, DNase I, β-mercaptoethanol, and IPTG were obtained from Sigma. *N*-laurylsarcosine, 10× solubilization buffer solution, plasmid pET11a, and *E. coli* strain BL21(DE3) were obtained from Novagen.

Cloning and Expression of the E. coli FtsH and RpoH Genes. Primers from the *E. coli* rpoH gene (σ^{32}) (ccccatATGACTGAC AAAATGCAAAG) (cccggatccTTACGCTTCAATGGCAGCACGC) and the ftsH gene (ccccatATGGCGAAAAACCT AATAC) (cccagatctTTACTTGTCGCCTAACTGCTCT) were used to amplify the genes from *E. coli* total genomic DNA. Thermocycling parameters were as follows: one cycle at 95 °C for 5 min, followed by 30 cycles at 95 °C for 1 min, 55 °C for 2 min, and 72 °C for 1 min, and finally one cycle at 72 °C for 10 min. AmpliTaq DNA polymerase (Perkin-Elmer) was used. The PCR gene fragments were digested with the appropriate enzymes (New England Biolabs), purified from a 1% agarose gel (Qiagen), ligated into pET11a previously digested with *Nde1* and *BamH1*, and transformed into chemically competent *E. coli* DH5α (Gibco BRL). Gene sequences were confirmed by DNA sequence analysis. Plasmids were transformed into *E. coli* BL21(DE3) for expression.

Purification of σ^{32}. The purification protocol is a modification of existing protocols (*34*, *35*). Cells containing the σ^{32} expression construct were grown at 28 °C in 350 mL of LB media plus 100 μg/mL ampicillin. Expression was induced by addition of IPTG to 1 mM for 60 min. The culture was centrifuged at 10 000*g* for 20 min. Cells were resuspended in 40 mL of BPER plus protease cocktail 2 (as per manufacturer's instructions) and frozen at −80 ° C. Cells were thawed, shaken gently at room temperatue for 20 min, and centrifuged for 30 min at 47 000*g*. To 39 mL of cleared lysate, 13.65 g of solid ammonium sulfate (55% saturation) was added slowly with stirring over 30 min. The suspension was stored overnight at 4 °C. Precipitate was collected by centrifugation at 47 000*g* for 30 min. Pellets were washed with buffer A (50 mM Tris-HCl pH 8.5, 10% glycerol, 0.5 mM EDTA) 55% saturated with ammonium sulfate. Pellets were resuspended in 100 mL of buffer A containing 6 mM β-mercaptoethanol and protease inhibitor cocktail 2. Protein was loaded on a 10 mL Q-Sepharose Fast-Flow column

[1] Abbreviations: NTP, nucleoside-5′-triphosphate; IPTG, isopropyl β-D-thiogalactopyranoside; DTT, dithiothreitol; BPER, bacterial protein extraction reagent; TFA, trifluoroacetic acid.

equilibrated in buffer A at 0.4 mL/minute. The column was washed with 20 mL of buffer A, and protein was eluted with 30 mL of 400 mM NaCl in buffer A. σ^{32} protein was monitored by polyacrylamide gel electrophoresis, and fractions were pooled on this basis. The 30 mL eluate was diluted to 120 mL with buffer B (20 mM Hepes pH 7.3, 10% glycerol, 0.5 mM EDTA, 6 mM β-mercaptoethanol, and protease inhibitor cocktail 2) and loaded on a 10 mL (2−5 mL BioRad Econopak Heparin cartridges) column equilibrated in buffer B. The column was washed with 20 mL of buffer B containing 100 mM NaCl. Protein was eluted with a 20 bed volume linear gradient (200 mL) from 100 to 1000 mM NaCl in buffer B at 1 mL/min; 3 mL fractions were collected. Fractions containing σ^{32} were pooled (14.5 mL) and concentrated to 1.5 mL in a Centriprep 30 concentrator, aliquoted, and frozen at −80 °C. A yield of 3.8 mg of σ^{32} was obtained from 350 mL of culture.

Solubilization and Refolding FtsH. Cells containing the FtsH expression construct were grown at 28 °C in 750 mL of LB media plus 100 μg/mL ampicillin. FtsH expression was induced by addition of IPTG (1 mM) for 3 h. Cells were collected by centrifugation at 10 000*g* for 20 min, resuspended in 40 mL of BPER plus protease inhibitor cocktail 2, and frozen at −80 °C. Cells were thawed, and the following additions were made: 200 μL of 1 M $MgCl_2$, 40 μL of 1 M DTT, 40 μL of 100 mM $ZnCl_2$, 10 000 units of DNase I, and 8 mg of lysozyme. The mix was incubated at 22 °C for 45 min, then centrifuged at 47 000*g* for 30 min. Pellets were resuspended in 40 mL of 50 mM Tris-HCl pH 8.0, 1% (v/v) NP-40, 1 mM DTT, 5 mM $MgCl_2$, 100 μM $ZnCl_2$, and protease inhibitor cocktail 2; stirred gently at 4 °C for 30 min; and then centrifuged at 47 000*g* for 30 min. Pellets were resuspended in 40 mL of the same buffer containing 0.1% NP-40 for 30 min. The sample was divided into two equal portions and centrifuged. Each pellet was resuspended in 8.8 mL of solubilization buffer (1× Novagen solubilization buffer, 5 mM $MgCl_2$, 100 μM $ZnCl_2$, 1 mM DTT) at 22 °C. During solubilization and refolding, one sample contained 1 mM ATP, the other did not. To prevent formation of a cloudy precipitate, the following order of addition was made: 8.8 mL of solubilization buffer (1.0 mL of 10 mM ATP or 1.0 mL of water) and then 0.2 mL of 30% *N*-laurylsarcosine (0.6% final concentration). Mixtures were stirred gently at 22° for 30 min. Insoluble material was removed by centrifugation at 16 000*g* for 10 min. A total of 25 mL of renaturation buffer (50 mM Tris-HCl pH 8.0, 0.5% NP40, 5 mM $MgCl_2$, 100 μM $ZnCl_2$, and 1 mM DTT) ± 1 mM ATP was added 1 mL at a time over 30 min at 22 °C. The mixture was allowed to sit for 10 min, followed by addition of 25 mL of renaturation buffer ± 1 mM ATP over 10 min. A final 10 mL of renaturation buffer ± 1 mM ATP was added, and the mixture was placed on ice for 30 min, then dialyzed against 4 L of 25 mM Tris-HCl pH 8.5, 5 mM $MgCl_2$, 100 μM $ZnCl_2$, 0.1% NP40, and 1 mM DTT overnight at 4 °C. The 75 mL dialysates (fraction I) were centrifuged at 40 000*g* for 20 min. The minus ATP fraction was frozen for a later assay, as was an aliquot of the plus ATP fraction.

Purification of Refolded FtsH. The plus ATP fraction was loaded on a 30 mL Q-Sepharose Fast-Flow column equilibrated in buffer C (25 mM Tris-HCl pH 8.5, 5 mM $MgCl_2$, 100 μM $ZnCl_2$, 0.5% NP40, 1 mM DTT, and protease inhibitor cocktail 2) at 1 mL/min. The column was washed with 120 mL of buffer C. Protein was eluted with 1 M NaCl in buffer C (fraction II). FtsH was monitored by polyacrylamide gel electrophoresis, and fractions were pooled on this basis. Fractions containing FtsH (50 mL) were dialyzed overnight against 4 L of buffer D (10 mM potassium-phosphate pH 6.9, 5 mM $MgCl_2$, 10 μM $ZnCl_2$, 1 mM DTT, 0.1% NP-40). The dialysate was loaded on a 20 mL hydroxyapatite CHT-2 column and equilibrated in buffer D containing 0.5% NP-40 at 0.8 mL/min. The column was washed with 50 mL of buffer D (0.5% NP-40), and protein was eluted with a 10 bed volume linear gradient (200 mL) from 10 to 250 mM potassium-phosphate pH 6.9 in buffer D (0.5% NP-40) at 1 mL/min: 5 mL fractions were collected. FtsH containing fractions were pooled (21 mL) and dialyzed overnight against 2 L of 25 mM Tris-HCl pH 8.0, 5 mM $MgCl_2$, 10 μM $ZnCl_2$, 1 mM DTT, 0.1% NP-40 with one change of buffer (fraction III). Protein was concentrated in a Millipore centrifuge filter unit (30 kDa cutoff) to 4 mL, aliquoted, and frozen at −80 °C.

Gel Filtration of FtsH. Analytical amounts of FtsH were fractionated further by gel filtration on Superose 6. Fraction II, or fraction III (250 μL), was loaded on a 25 mL Superose 6 column equilibrated in 50 mM Tris-HCl pH 8.0, 5 mM $MgCl_2$, 10 μM $ZnCl_2$, 1 mM DTT, and 0.1% NP-40. The column was run at 0.2 mL/min, and 0.5 mL fractions were collected. Under these conditions, the peak of a homogeneous protein elutes over four to five fractions. Molecular weight markers included blue dextran (2000 kDa), thyroglobulin (669 kDa), apoferritin (443 kDa), β-amylase (200 kDa), alcohol dehydrogenase (150 kDa), and yellow dextran (25 kDa).

FtsH-Catalyzed Proteolysis. Hydrolysis of σ^{32} by FtsH-protease was monitored by a general method in which reaction mixtures are subjected to SDS−PAGE to separate σ^{32}-derived products from intact σ^{32}. In all cases, reactions were conducted at 42 °C and in a pH 8.0 buffer of the following composition: 50 mM Tris-HCl, 5 mM $MgCl_2$, 12.5 μM $ZnCl_2$, 80 mM NaCl, 1.4 mM β-mercaptoethanol, and 0.5% Brij 35 (v/v). Reaction progress was terminated by the addition of an equal volume of 2× Novex Tris-glycine SDS−PAGE buffer containing 5% (v/v) β-mercaptoethanol. Mixtures were heated to 95 °C and loaded onto a 4−20% gradient polyacrylamide gel in Tris-glycine buffer. Gels were stained with Coomassie brilliant blue. To quantify band intensities, gels were scanned on a flat-bed scanner at 600 dpi. Band intensities were determined with IP Lab Gel (Signal Analytics Corp.). To visualize the small (<3 kDa) proteolysis products, a more sensitive stain such as Gel Code Blue (Pierce) is required. As the linear range of this stain is limited, Coomassie brilliant blue was used for quantitating proteolysis reactions.

FtsH-Catalyzed Hydrolysis of Nucleotide Triphosphates. Hydrolysis of various NTPs by FtsH was determined by measuring phosphate evolution (*36*). Reaction of FtsH and NTP was conducted at 37 °C in 20 μL of a pH 8.0 buffer containing 50 mM Tris-HCl, 5 mM $MgCl_2$, 12.5 μM $ZnCl_2$, 80 mM NaCl, 1.4 mM β-mercaptoethanol, and 0.1% Brij-35 (v/v). Reaction was initiated by the addition of NTP. After 10 min, 250 μL of ammonium molybdate-malachite green reagent was added. After a development time of 1 min, 30 μL of 34% citric acid (w/v) was added. Absorbance was read

at 650 nm. Ammonium molybdate-malachite green reagent consists of a 3:1 mixture of 0.045% malachite green hydrochloride (w/v)/4.2% ammonium molybdate (w/v) in 4 N HCl.

FtsH-Catalyzed Peptide Hydrolysis. Hydrolysis of Phe-Gly-His-^{NO_2}Phe-Phe-Ala-Phe-OMe (Bachem) was monitored by an HPLC-based method. All reactions were conducted at 42 °C for 10 min in 100 μL of a pH 8.0 buffer containing 50 mM Tris-HCl, 5 mM $MgCl_2$, 12.5 μM $ZnCl_2$, 80 mM NaCl, 1.4 mM β-mercaptoethanol, 0.5% Brij 35, at 25 nM FtsH and various concentrations of ATP and peptide. Reactions were initiated by the addition of ATP and quenched by the addition of 10 μL of 0.5 M EDTA. Reaction products were separated from intact substrate and ATP by reverse phase chromatography on a Waters Millennium HPLC system. A total of 100 μL of quenched reaction mix was injected onto a Waters C_{18} Nova-Pak column that had been equilibrated in 10% acetonitrile/0.1% TFA. Column elution was with a gradient from 10 to 70% acetonitrile in 0.1% TFA over 12 min at a flow rate of 1 mL/min. Detection was based on the 310 nm absorbance of the *p*-nitrophenyl moiety of the substrate and one reaction product, Phe-Gly-His-^{NO_2}Phe. A series of known substrate concentrations were run to obtain a standard curve.

FtsH-Catalyzed Peptide and ATP Hydrolysis. FtsH was incubated with ATP and various concentrations of Phe-Gly-His-^{NO_2}Phe-Phe-Ala-Phe-OMe. All reactions were conducted at 42 °C in 700 μL of a pH 8.0 buffer containing 50 mM Tris-HCl, 5 mM $MgCl_2$, 12.5 μM $ZnCl_2$, 80 mM NaCl, 1.4 mM β-mercaptoethanol, 0.1% Brij 35, at 180 nM FtsH and 200 μM ATP. The 100 μL aliquots were withdrawn at 3, 6, 9, 12, and 15 min. Reactions were quenched by the addition of 10 μL of 0.5 M EDTA. Phosphate concentration (in 20 μL) was determined by the malachite green assay as described above. Peptide reaction products (in 50 μL) were separated from intact substrate and ATP by reverse phase HPLC and quantitated as described above.

RESULTS

Solubilization, Refolding, and Purification of FtsH Protease. Genes encoding FtsH and σ^{32} (rpoH) were cloned into the expression vector pET11a. Induction with IPTG produced a high level of expression of each protein. σ^{32} was easily purified by a modification of existing protocols (*34*, *35*). Attempts to extract soluble FtsH from a crude *E. coli* membrane fraction were unsuccessful; even high concentrations (5% v/v) of the nonionic detergent NP-40 failed to solubilize FtsH protein. The crude membrane preparation was fractionated by centrifugation in a sucrose step-gradient (*37*, *38*). FtsH was not in the membrane fraction, rather, it was found in the pellet. These results indicate that FtsH had formed inclusion bodies. A systematic alteration of induction conditions failed to produce NP-40-extractable FtsH protein.

We were able to achieve an effective solubilization of FtsH from its inclusion bodies using the ionic detergent, *N*-laurylsarcosine. As indicated in the previous section, FtsH was solubilized in a solution of 0.6% *N*-laurylsarcosine (v/v) that contained Mg^{2+} and Zn^{2+} cations as well as ATP. *N*-laurylsarcosine was diluted out by the slow, sequential addition of a 0.5% NP-40 solution containing Mg^{2+}, Zn^{2+}, and ATP. Following dialysis, the protein was found to have both ATP- and CTP-dependent proteolytic activity against σ^{32}. In contrast, FtsH protein refolded in the absence of ATP had only 15% of the proteolytic activity of the protein refolded with ATP (Table 1). EDTA and *o*-phenanthroline both inhibited FtsH proteolytic activity (data not shown). Inhibitors of other classes of proteases, such as phenylmethylsulfonylfluoride, had no effect on FtsH activity (data not shown).

Table 1: Purification of Recombinant Refolded FtsH[a]

purification procedure	volume (mL)	total protein (mg)	total activity (nmol of σ^{32}/min)	specific activity (nmol of σ^{32}/min/mg)
fraction I refolded FtsH − ATP	75	55	8.3	0.15
fraction I refolded FtsH + ATP	75	55	55	1.0
fraction II fast flow Q sepharose	50	41	45	1.1
fraction III hydroxyapatite CHT-2	21	8.2	30	3.6

[a] Details of each purification step are given in Experimental Procedures. Each protein fraction was incubated with σ^{32} as described; to obtain initial rates, a 10 min time course was run.

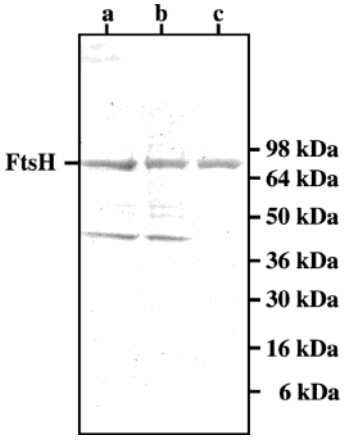

FIGURE 1: Purification of recombinant refolded FtsH. Protein fractions: (a) fraction I, FtsH refolded in the presence of ATP; (b) fraction II, Fast-Flow Q-Sepharose; and (c) fraction III, hydroxyapatite-CHT-2.

N-laurylsarcosine has been used as an alternative to denaturants such as guanidine-HCl to solublize proteins from inclusion bodies (*32*, *33*). The rationale for our refolding scheme is as follows: when FtsH is solubilized with *N*-laurylsarcosine, the transmembrane regions of FtsH should insert into the detergent micelle. As *N*-laurylsarcosine is diluted out with NP-40, the adjacent ATP-binding domain will refold around Mg^{2+}-ATP. As the *N*-laurylsarcosine concentration is reduced further, the rest of the protein will refold around the Zn^{2+}-binding domain. Free *N*-laurylsarcosine and ATP are removed by dialysis, leaving mixed *N*-laurylsarcosine−NP-40 micelles.

FtsH protein was applied to Fast-Flow Q-Sepharose and washed extensively with low ionic strength buffer containing NP-40 to exchange detergents. ATP-dependent proteolytic activity was eluted with 1 M NaCl. The major protein band in this fraction had a molecular weight of approximately 70 kDa, corresponding to that expected for FtsH. FtsH was

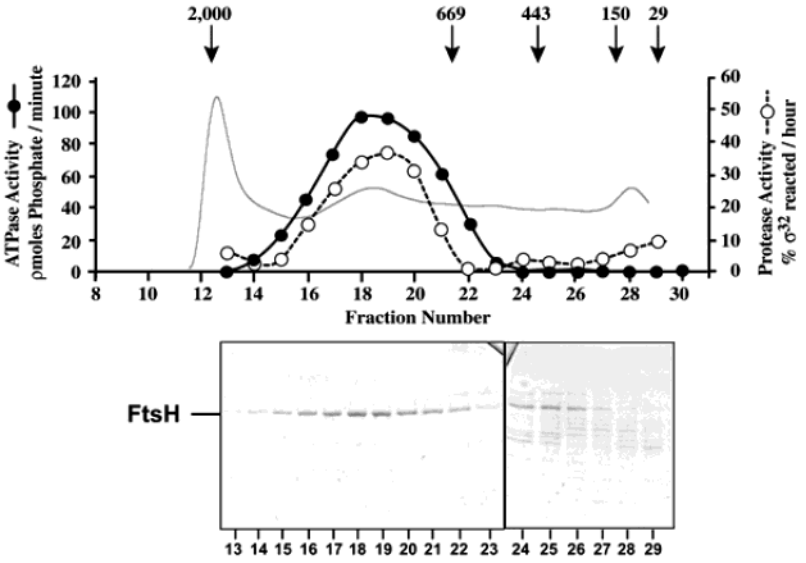

FIGURE 2: Gel Filtration of FtsH. FtsH (fraction II) was fractionated on Superose 6: (a) (−) trace of UV absorbance at 254 nm, (●) ATPase activity of Superose 6 fractions, (○) proteolytic activity of Superose 6 fractions vs σ^{32}. A total of 15 μL of each fraction was incubated with 5 mM ATP at 37° for 10 min. Reaction conditions, and phosphate determination, are as described in Experimental Procedures. A total of 15 μL of each fraction was incubated at 42° with σ^{32} for 60 min. Reaction conditions, and determination of the extent of σ^{32} conversion, are as described in Experimental Procedures. Position of elution of molecular weight markers (in kDa) indicated by vertical arrows. (b) SDS−PAGE of Superose 6 fractions.

purified further by chromatography on hydroxyapatite, resulting in a fraction that was >95% FtsH protein (Figure 1). The protocol yielded 22 mg of purified FtsH protein/L of *E. coli* culture. The specific activity, 3.6 nmol of σ^{32}/min/mg of FtsH, is comparable to the previously reported value of 2.9 nmol of σ^{32}/min/mg of FtsH (*8*).

Size-Exclusion Chromatography of FtsH. The specific-activity for σ^{32} proteolysis in fraction II is 3.3-fold lower than fraction III (Table 1). The ATPase activity is 3-fold lower as well (data not shown). However, both protein fractions consist mostly of a band at 70 kDa (Figure 1). Gel filtration of fraction III on Superose 6 yields a discrete peak of FtsH centered at 1200 kDa (data not shown).

Following the gel filtration of fraction II, FtsH fractionated over a wide range of molecular weights. Proteolytic reactions with σ^{32} and ATPase reactions were performed on these fractions (Figure 2a). The peak of proteolytic activity was coincident with the peak of ATPase activity and a peak of FtsH (Figure 2b) centered at 1200 kDa. Only the large complex had ATPase and proteolytic activities.

It is not possible to unambiguously predict the size of a hexameric FtsH−NP-40 micelle system. With an NP-40 micelle size of 90 kDa, the FtsH (70 kDa) monomer−detergent complex, if molecular weights are simply additive, would elute at a position corresponding to 160 kDa. The apparent MW of a multimer in solution depends on the packing of the subunits and arrangement of the detergent micelles.

Nucleoside-5′-triphosphate-Dependent Proteolytic Activity of FtsH. FtsH was incubated with σ^{32} and a variety of NTPs. No degradation of σ^{32} was observed in the absence of NTP. Addition of ATP or CTP to the reaction resulted in the degradation of σ^{32} (Figure 3), while no degradation was observed in the presence of GTP or UTP (data not shown). Likewise, dATP and dCTP supported FtsH proteolysis of σ^{32} (Figure 3), while dGTP and TTP did not (data not shown).

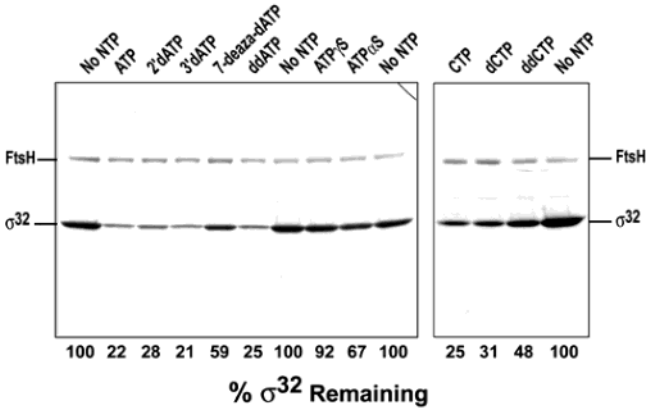

FIGURE 3: Specificity of FtsH toward NTPs. 2 μM FtsH monomer was incubated with 16 μM σ^{32} for 60 min at 42 °C in the presence of 5 mM indicated NTP (except 7-deaza-dATP, 2.5 mM). The number at the bottom of the gel indicates the percent of σ^{32} remaining after 60 min.

A series of synthetic ATP and CTP analogues was also tested (Figure 3). Both 2′ and 3′ deoxy-ATP as well as 2′,3′ dideoxy-ATP supported hydrolysis of σ^{32} by FtsH. 7-Deaza-2′-deoxy-ATP supported FtsH proteolysis of σ^{32} but to a lesser extent. Dideoxy CTP also supported proteolysis by FtsH. Finally, ATPγS did not support FtsH proteolysis, while ATPαS did to a limited extent.

Significantly, hydrolysis of σ^{32} by 2 μM FtsH appears to proceed by a mechanism that produces no intermediates at any time points (Figure 3). Instead, all that can be observed is a cluster of small fragments of a molecular mass less than about 3 kDa at the bottom of the gel (data not shown, see Experimental Procedures). Thus, FtsH appears to processively degrade σ^{32}; once substrate is bound neither it nor any intermediates are released.

Determination of Steady-State Kinetic Parameters for Hydrolysis of σ^{32} by FtsH. At σ^{32} concentrations that ranged from 1 to 32 μM, reaction progress curves were determined for hydrolysis by 2 μM FtsH monomer. From these curves,

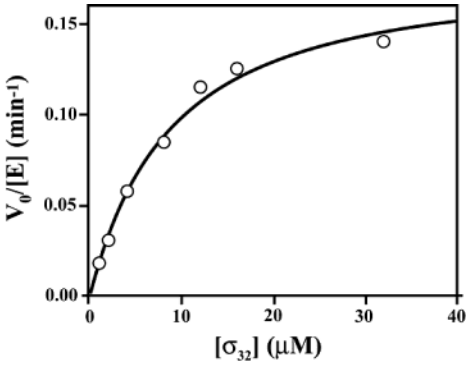

FIGURE 4: Substrate concentration dependence of initial velocities for the FtsH-catalyzed hydrolysis of σ^{32}. Progress curves for substrate consumption were determined for the reaction of 2 μM FtsH monomer and the indicated concentration of σ^{32}. Steady-state velocities were calculated from the initial portions of these curves and plotted vs σ^{32} concentration.

Table 2: Steady-State Kinetic Parameters for FtsH-Catalyzed Hydrolysis of Nucleoside-5′-triphosphates[a]

NTP	k_c (min^{-1})	K_m (μM)	k_c/K_m (mM^{-1} min^{-1})
ATP	18 ± 1	23 ± 3	780
CTP	19 ± 1	104 ± 10	180
GTP	32 ± 5	7300 ± 2000	4
ATP[b]	14 ± 1	21 ± 3	670

[a] Steady-state kinetic parameters were detemined from the fit of the dependence of initial velocities on NTP concentration to the Michaelis−Menten equation. Error limits are from the fitting procedure. Reaction conditions: 50 mM Tris-HCl, pH 8.0, 5 mM $MgCl_2$, 12.5 μM $ZnCl_2$, 80 mM NaCl, and 1.4 mM β-mercaptoethanol; T = 37 °C; [FtsH] = 200 nM (fraction III). [b] In this experiment, [Phe-Gly-His-^{NO_2}Phe-Phe-Ala-Phe-OMe] = 50 μM = 4K_m.

initial velocities were calculated and plotted versus substrate concentration (see Figure 4). The dependence of velocity on substrate concentration can be fit to the Michaelis−Menten equation to yield the following parameters: $k_c = 0.18 \pm 0.01$ min^{-1} and $K_m = 8.5 \pm 1.2$ μM.

Determination of Steady-State Kinetic Parameters for Hydrolysis of Nucleoside-5′-triphosphates by FtsH. Preliminary experiments indicated that the specific ATPase activity of fraction III was 193 nM P_i/min/mg of FtsH and comparable to the previously reported value of 223 nM P_i/min/mg of FtsH (*8*). Initial velocities of inorganic phosphate production were measured for the FtsH-catalyzed hydrolyses of ATP, CTP, and GTP. In all cases, the dependence of the reaction rate on NTP concentration could be fit to the Michaelis−Menten equation and provided the steady-state kinetic parameters that are summarized in Table 2.

A question of some mechanistic importance is whether the kinetics of ATP hydrolysis is regulated in any way by the protein substrate. We examined this problem by use of the peptide substrate Phe-Gly-His-^{NO_2}Phe-Phe-Ala-Phe-OMe at a concentration of peptide substrate of 50 μM (= 4K_m). At this concentration, k_c for ATP hydrolysis is 30% lower than the control. The decrease in k_c could be due to a reduction in uncoupled ATP hydrolysis during proteolysis.

The properties of refolded FtsH protein, ATP or CTP-dependent proteolytic activity, specific activity of proteolysis of σ^{32}, specific activity and K_m for ATP, and formation of a large multimeric complex gave us confidence that our enzyme preparation had the appropriate activities and thus could be used for detailed kinetic and mechanistic studies.

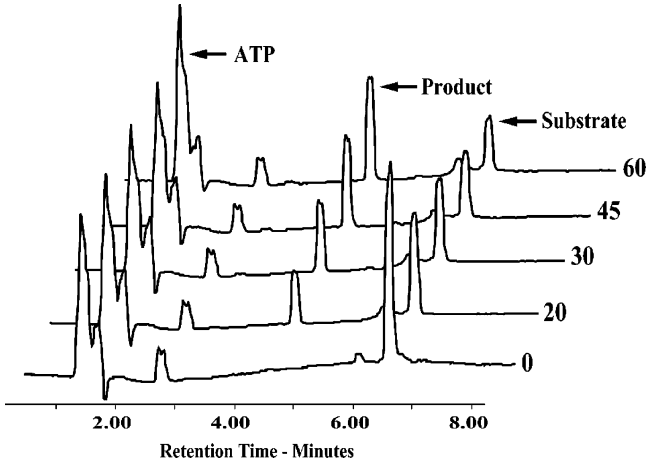

FIGURE 5: Time course of FtsH hydrolysis of a peptide substrate. In the presence of ATP, FtsH cleaves Phe-Gly-His-^{NO_2}Phe-Phe-Ala-Phe-OMe on the C-terminal side of pNO_2-phenylalanine. FtsH (200 nM) was incubated with peptide (20 μM) at 42° C, and reaction conditions were as described in Experimental Procedures. Reaction was initiated by addition of 200 μM ATP, and aliquots were withdrawn at time points between 0 and 60 min (indicated by the number to the right of each trace) and quenched with EDTA. Product was separated from substrate by reverse phase-HPLC as described in Experimental Procedures.

Kinetic Mechanism of FtsH-Catalyzed ATP-Dependent Peptide Hydrolysis. Monitoring the hydrolysis of σ^{32} by FtsH by gel electrophoresis is cumbersome and imprecise. In addition, disappearance of the entire protein, which involves a number of proteolytic cleavages, is what is determined experimentally. The substrate is heterologous, and FtsH may not clip the protein at the same position each time but rather a distribution of products may occur. Additionally, the substrate must be unwound before it can be proteolyzed. These factors make detailed kinetic analysis of FtsH proteolysis on a protein substrate difficult. Use of a peptide substrate would allow us to study the kinetics of the translocation and proteolysis phases of the reaction.

Recent work (*39*) demonstrated that an FtsH homologue from *Thermus thermophilus* HB8 cleaves on the C-terminal side of hydrophobic residues in α-casein and pepsin. With this latter piece of information in mind, we tested several commercially available peptides that have internal Phe residues. The most efficiently hydrolyzed peptide is Phe-Gly-His-^{NO_2}Phe-Phe-Ala-Phe-OMe. Our preliminary experiments demonstrated that the hydrolysis of this peptide by FtsH has an absolute dependence on the presence of NTP, and in the presence of 5 mM ATP, CTP, or GTP, it is hydrolyzed at one position only to produce a single ^{NO_2}Phe-containing product (Figure 5). Mass spectral analysis of this product identified it as Phe-Gly-His-^{NO_2}Phe and confirmed exclusive cleavage of the peptide at the ^{NO_2}Phe−Phe bond. Significantly, ATPγS cannot substitute for ATP in this reaction; a hydrolyzable NTP analogue appears to be required. And, unlike σ^{32} where no degradation was observed, the peptide substrate can be cleaved by FtsH in the presence of 5 mM GTP.

To begin our exploration of how ATP regulates peptide hydrolysis, we determined the dependence of peptide hydrolytic rates on peptide concentration at 11 fixed concentra-

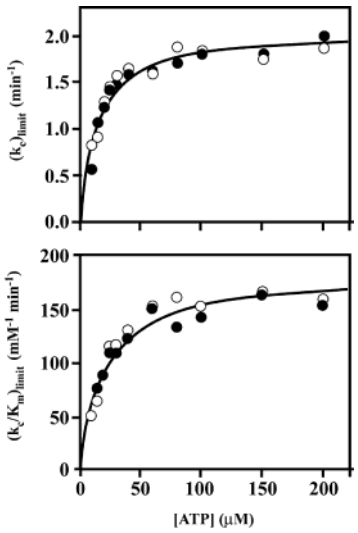

FIGURE 6: Kinetic analysis of FtsH with peptide substrate. FtsH reactions were run in duplicate at 11 ATP concentrations and eight peptide concentrations. At a given concentration of ATP, initial velocity data for each peptide concentration was fitted to the Michaelis−Menten equation, and K_m and k_c were determined. (a) Plot of k_c for peptide as a function of [ATP]; (b) plot of k_c/K_m for peptide as a function of [ATP].

tions of ATP that ranged from 10 to 200 μM. In all cases, the dependence of reaction rate on peptide concentration, which ranged from 5 to 100 μM, fit well to the Michaelis−Menten equation to provide the observed, ATP-dependent values of k_c and k_c/K_m, which are plotted as a function of [ATP] in Figure 6.

Both k_c and k_c/K_m show a simple hyperbolic dependence on ATP concentration and can be fit to the expression of eq 1:

$$k_{obs} = \frac{k_{limit}[ATP]}{K_{ATP} + [ATP]} \quad (1)$$

For the dependence of k_c on [ATP], $(k_c)_{limit} = 2.1 \pm 0.1$ min^{-1} and $K_{ATP} = 12 \pm 2$ μM, while for the dependence of k_c/K_m on [ATP], $(k_c/K_m)_{limit} = 183 \pm 6$ mM^{-1} min^{-1}and $K_{ATP} = 19 \pm 2$ μM. A mechanism that incorporates all of these findings is later developed.

FtsH-Catalyzed ATP and Peptide Hydrolysis. FtsH was incubated with ATP (200 μM, 10K_m) and various concentrations of peptide substrate Phe-Gly-His-^{NO_2}Phe-Phe-Ala-Phe-OMe. Aliquots were withdrawn at indicated time points, and the reaction was quenched with EDTA. Phosphate evolution and peptide hydrolysis were determined. The ratio of ATP to peptide hydrolysis for each concentration of peptide was then calculated (Table 3).

As the concentration of the peptide increases, the rate of ATP hydrolysis decreases (reduced by 27% at 100 μM peptide, as compared to zero peptide). As expected, the rate of peptide hydrolysis increases as the concentration approaches saturation. Overall, the ratio of ATP to peptide hydrolysis decreases as peptide concentration increases. Thus, the peptide hydrolysis reaction becomes more efficient with respect to ATP hydrolysis, as peptide increases. At a concentration of 8K_m for peptide, the ratio of ATP to peptide hydrolysis is 8.3, approaching the model's predicted value of 6 (*30*).

Table 3: Ratio of ATP to Peptide Hydrolysis by FtsH[a]

peptide (μM)	ATPase (min^{-1})	peptide hydrolysis (min^{-1})	ratio (ATP/peptide)
0	21.8 ± 1.44		
12.5 (K_m)	20.2 ± 1.48	1.12 ± 0.083	18.0
25 (2K_m)	19.4 ± 0.57	1.53 ± 0.036	12.7
50 (4K_m)	17.5 ± 1.17	1.62 ± 0.117	10.8
100 (8K_m)	15.9 ± 0.76	1.92 ± 0.174	8.3

[a] FtsH (180 nM) was incubated with ATP (200 μM) and various concentrations of Phe-Gly-His-^{NO_2}Phe-Phe-Ala-Phe-OMe at 42 °C. At 3 min intervals, aliquots were withdrawn and quenched with EDTA. The extent of ATP and peptide hydrolysis were determined as described in Experimental Procedures. Plots of ATP hydrolyzed vs time, and peptide hydrolyzed vs time, were fitted by linear regression to obtain rates. Error limits are from the fitting procedure.

DISCUSSION

In this paper, we describe a high-yield protocol for the solubilization, refolding, and purification of FtsH. This refolded protein has properties identical to those reported previously for detergent-solubilized FtsH (*8*), including: (i) ATP- or CTP-dependent proteolytic activity with protein substrate σ^{32}; (ii) specific activity of σ^{32} degradation; (iii) formation of a large homo-oligomeric complex; and (iv) kinetics of ATP hydrolysis. In addition, we have demonstrated that only the large 1200 kDa complex of FtsH possesses proteolytic and ATPase activities; these activities are not found in smaller forms. Finally, we have developed a peptide-based assay for use in kinetic analysis of FtsH proteolytic activity.

Solubilization, Refolding, and Purification of FtsH. The refolding and purification protocol described typically yields 20−25 mg of FtsH per liter of *E. coli* culture. High concentrations of nonionic detergent (5% NP-40) did not solubilize any ATP-dependent proteolytic activity. This detergent concentration is enough to completely disrupt the membrane. Since FtsH is found in the pellet following relatively low *g* force centrifugation after detergent extraction, and is found in the pellet upon sucrose gradient centrifugation of a crude membrane fraction, we conclude that overexpressed FtsH is in inclusion bodies. Inclusion of ATP in solubilization and refolding solutions increases the proportion of active FtsH dramatically. In addition to refolding, it is possible that ATP binding assists in the assembly of FtsH into higher-order structures, as observed in other AAA proteins, such as the Large T-antigen of SV-40 virus (*40*).

The purification of FtsH from inclusion bodies consists of cell lysis, separation of soluble proteins, and extraction of membrane proteins with NP-40. After solubilization with *N*-laurylsarcosine and refolding, the bulk of the remaining protein is FtsH. Purification is required mainly to separate the higher molecular weight active form of the protein from the lower molecular weight inactive species. Enough FtsH can be produced economically to supply protein for high-throughput screening and mechanistic and structural studies. This extraction and refolding protocol may be applicable to the production of large quantities of other overexpressed membrane proteins.

Specificity of FtsH toward Nucleoside Triphosphate Substrates. FtsH can utilize a wide range of nucleoside-5′-triphosphate analogues to catalyze proteolysis. It is probable

that a number of contacts between FtsH and the NTP contribute to binding, of which only a hydrolyzable phosphate at the γ-position appears to be essential.

Many ATPases strictly require ATP; even dATP works poorly as a substitute. A notable exception are the translocases, ATPases that catalyze a physical movement, such as DNA and RNA helicases. The AAA protein T-antigen of SV-40 can use UTP as well as ATP to catalyze DNA unwinding from the SV-40 origin of replication (*41*). Another DNA-dependent helicase with similar NTP specificity to FtsH, UL9 of herpes simplex virus-1, can hydrolyze ATP, dATP, CTP, and dCTP (*42*). Since the NTPase specificity of FtsH is shared by only a small number of ATPases, it may be possible to design specific inhibitors of the ATPase activity of FtsH.

Kinetic Mechanism for FtsH. The results of our experiments suggest that FtsH catalyzes the hydrolysis of σ^{32} by a processive mechanism that liberates no intermediate species into solution. Our steady-state kinetic analysis of substrate consumption allows us to calculate the following observed rate constants: $k_c = 0.18$ min^{-1}, $K_m = 8.5$ μM, and $k_c/K_m = 21$ nM^{-1} min^{-1}.

Given the processive nature of catalysis by FtsH, it is important to consider how these observed rate constants relate to the actual microscopic rate constants for protein hydrolysis. The simplest processive mechanism that is consistent with our data is shown in Scheme 2 in which FtsH is designated E and σ^{32} is designated X_n, a linear polymer of n peptide fragments X. According to this mechanism, after FtsH binds σ^{32}, it sequentially unwinds the protein and cleaves off susceptible peptide fragments until the entire protein has been degraded. For such a mechanism, the following expressions relate the observed steady-state kinetic parameters to the mechanistic parameters of Scheme 2:

$$\frac{k_c}{K_m} = \frac{k_{Xn}}{K_s} \tag{2}$$

$$k_c = \{\sum_{i=2}^{n}(k_{Xi})^{-1}\}^{-1} \tag{3}$$

$$K_m = K_s\frac{\{\sum_{i=2}^{n}(k_{Xi})^{-1}\}^{-1}}{k_{Xn}} \tag{4}$$

In the mechanism of Scheme 2, k_{Xn} governs the first irreversible step; thus, k_c/K_m is simply k_{Xn}/K_s, as shown in eq 2, and reflects the free energy barrier between enzyme and substrate free in solution and the transition state for k_{Xn}. For the series of irreversible steps that comprise substrate turnover, k_c will be dominated by the step with the largest energy barrier and is equal to the reciprocal of the sum of reciprocals of the individual rate constants k_{Xi}. From this expression, it can be seen that if one step is much slower than the rest, k_c will be numerically equal to the rate constant for this step. As always, K_m is the ratio of k_c to k_c/K_m and equals the expression of eq 4. From this expression, it can be seen that K_m reflects the most stable enzyme:substrate species that accumulates in the steady-state. And, of course, this species need not be the initial Michaelis complex $E:X_n$.

Scheme 2: Processive Mechanism for Protein Hydrolysis by FtsH

$$E + X_n \underset{K_s}{\rightleftharpoons} E{:}X_n$$

$$E{:}X_n \xrightarrow{k_{X_n}} E{:}X_{n-1} + X$$

$$E{:}X_{n-1} \xrightarrow{k_{X_{n-1}}} E{:}X_{n-2} + X$$

$$\vdots$$

$$E{:}X_2 \xrightarrow{k_{X_2}} E + 2X$$

Scheme 3: Minimal Mechanism for FtsH-Catalyzed ATP and Peptide Hydrolysis

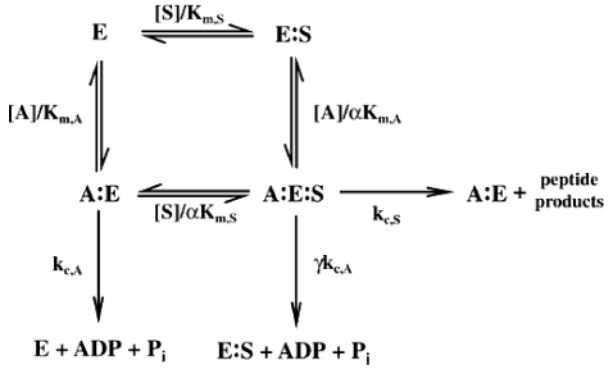

For σ^{32}, n is approximately 10 since σ^{32} has a molecular mass of 32 kDa and is degraded into fragments each having a mass less of than 3 kDa. If we assume that the k_{Xn} values for the nine sequential cleavage reactions are the same, then a rearranged form of eq 3, together with the observed k_c of 0.2 min^{-1}, allows us to calculate $k_{Xn} = 1.8$ min^{-1}, which is essentially identical to the k_c of 2.1 min^{-1} value for hydrolysis of Phe-Gly-His-^{NO_2}Phe-Phe-Ala-Phe-OMe by FtsH. However, comparisons between peptide and protein substrates must be made with caution, in light of the fact that σ^{32} proteolysis requires the additional step of unwinding the substrate prior to translocation and peptide bond cleavage.

To gain an understanding of how ATP and its hydrolysis regulate the proteolytic activity of FtsH, we examined the ATP-dependent hydrolysis of Phe-Gly-His-^{NO_2}Phe-Phe-Ala-Phe-OMe. The minimal mechanism that can account for our data is shown in Scheme 3. According to this mechanism, the enzyme can bind either peptide or ATP to form binary complexes having dissociation constants $K_{m,S}$ and $K_{m,A}$, respectively. While the hydrolysis of ATP can occur from within either A:E or A:E:S, hydrolysis of the peptide occurs only from within A:E:S; the binary Michaelis complex E:S is not catalytically competent. Note that while thermodyanics requires the existence of E:S, we have directly detected its presence. The fact that α is around 0.6 supports the presence of E:S in the steady-state and random mechanism as shown in Scheme 3.

We can estimate the rate constants of Scheme 3 from our steady-state kinetic analysis in the following way. From the [ATP] dependence of k_c/K_m for peptide hydrolysis, a K_{ATP} value of 19 μM was determined that is identical to $K_{m,A}$ of Scheme 3. Likewise, from the [ATP] dependence of k_c for

Scheme 4: Coupling of ATP Hydrolysis to Peptide Hydrolysis during the Catalytic Cycle of FtsH

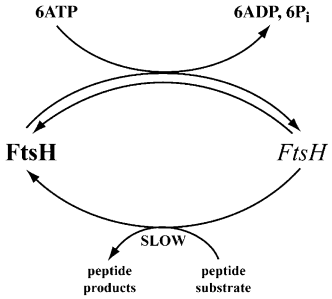

peptide hydrolysis, a K_{ATP} value of 12 μM was determined that is identical to $\alpha K_{m,A}$. These values of $K_{m,A}$ and $\alpha K_{m,A}$ allow us to calculate an α value of 0.63. From this same analysis, the values of $(k_c)_{limit}$ and $(k_c/K_m)_{limit}$ that we determined for peptide hydrolyis allow us to calculate $(K_m)_{limit} = \alpha K_{m,S} = 13$ μM; thus, $K_{m,S} = 21$ μM. The data of Table 3 provide $k_{c,A} = 22$ min^{-1} and $\gamma k_{c,A} = 16$ min^{-1}. Finally, $(k_c)_{limit} = k_{c,S} = 2.1$ min^{-1}.

It is a curious and potentially significant observation that the ratio of turnover numbers for ATP and peptide hydrolysis from the ternary A:E:S complex is 8.3. This ratio approaches the number of FtsH subunits that are proposed to comprise its hexameric active structure and suggests a number of intriguing mechanisms for the coupling of ATP and peptide hydrolysis. Since this ratio of 8.3 cannot be explained based on arguments relating to the innate chemical reactivity of ATP and the peptide toward hydrolytic cleavage, all these mechanisms must propose that at least one of these hydrolytic events is rate-limited by a conformational isomerization of the FtsH.

A mechanism that we favor is shown in Scheme 4. According to this mechanism, a conformer of enzyme, FtsH, binds and hydrolyzes six molecules of ATP to ADP and P_i. During the course of ATP hydrolysis, FtsH undergoes an isomerization to *FtsH*, an isomer that either returns to FtsH or binds and hydrolyzes the peptide substrate. Hydrolysis of peptide and release of peptide products is accompanied by isomerization of *FtsH* to FtsH. This mechanism explains the observed turnover number ratio of 8.3 as well as the ability of FtsH to hydrolyze ATP in the absence of peptide substrate and the absolute requirement for ATP hydrolysis during peptide hydrolysis.

Relation to Structural Studies. In a recently reported model (*30*), FtsH forms a ring structure with a hollow core. ATP and protease active sites are located in domains of FtsH subunits. Interaction between them would probably be through a conformational shift during ATP hydrolysis (see Scheme 4). ATP hydrolysis causes the inner portions of the hexameric torus to flex open and closed like an iris. This flexing of the central core triggers a conformational change that serves to unwind and translocate protein substrates to the protease active sites. The model predicts that hydrolysis of six ATPs is sufficient to translocate a peptide through the complex. Like other translocases, ATP hydrolysis would be used to ensure spatial directionality of the proteolytic processing; the proteolysis reaction per se does not require an input of energy. In the absence of substrate, an uncoupled ATPase reaction could occur. With substrate occupying the central core, a conformational change caused by ATP hydrolysis might be restricted due to steric interactions, and uncoupled ATP hydrolysis would be reduced.

This structural and mechanistic proposal for FtsH is supported by the results of our study: (i) Active FtsH is a large complex (1200 kDa); smaller forms have no protease or ATPase activity. (ii) Proteolysis of σ^{32} is processive; no proteolytic intermediates are observed. (iii) There is communication between ATPase and protease sites. (iv) k_c for ATP decreases in the presence of saturating peptide substrate, while K_m is unchanged and the dissociation constant for ATP is lower when peptide is bound to enzyme. (v) A hydrolyzable NTP is an absolute requirement for the processing of both protein and peptide substrates.

ACKNOWLEDGMENT

We gratefully acknowledge A. M. Smallwood for constructing the figures and for helpful discussions during the course of these studies and M. J. Haas for performing mass spectral analysis.

REFERENCES

1. Ogura, T., Tomoyasu, T., Yuki, T., Morimura, S., Begg, K. J., Donachie, W. D., Mori, H., Niki, H., and Hiraga, S. (1991) *Res. Microbiol. 142*, 279−282.
2. Tomoyasu, T., Yuki, T., Morimura, S., Mori, H., Yamanaka, K., Niki, H., Hiraga, S., and Ogura, T. (1993) *J. Bacteriol. 175*, 1344−1351.
3. Schumann, W. (1999) *FEMS Microbiol. Rev. 23*, 1−11.
4. Ogura, T., Inoue, K., Tatsuta, T., Suzaki, T., Karata, K., Young, K., Su, L. H., Fierke, C. A., Jackman, J. E., Raetz, C. R. H., Colman, J., Tomoyasu, T., and Matsuzawa, H. (1999) *Mol. Microbiol. 31*, 833−844.
5. Nilsson, D., Lauridsen, A. A., Tomoyasu, T., and Ogura, T. (1994) *Microbiology 140*, 2601−2610.
6. Ge, Z., and Taylor, D. E. (1996) *J. Bacteriol. 178*, 6151−6157.
7. Anilkumar, G., Chauhan, M. M., and Ajitkumar, P. (1998) *Gene 214*, 7−11.
8. Tomoyasu, T., Gamer, J., Bukau, B., Kanemori, M., Mori, H., Rutman, A. J., Oppenheim, A. B., Yura, T., Yamanaka, K., Niki, H., Hiraga, S., and Ogura, T. (1995) *EMBO J. 14*, 2551−2560.
9. Herman, C., Ogura, T., Tomoyasu, T., Hiraga, S., Akiyama, Y., Ito, K., Thomas, R., D'Ari, R., and Bouloc, P. (1993) *Proc. Natl. Acad. Sci. U.S.A. 90*, 10861−10865.
10. Kihara, A., Akiyama, Y., and Ito, K. (1996) *EMBO J. 15*, 6122−6131.
11. Akiyama, Y., Kihara, A., Tokuda, H., and Ito, K. (1996) *J. Biol. Chem. 271*, 31196−31201.
12. Akiyama, Y., Kihara, A., and Ito, K. (1996) *FEBS Lett. 399*, 26−28.
13. Suzuki, C. K., Rep, M., Maarten van Dijl, J., Suda, K., Grivell, L. A., and Schatz, G. (1997) *Trends Biochem. Sci. 22*, 118−123.
14. Akiyama, Y., Ogura, T., and Ito, K. (1994) *J. Biol. Chem. 269*, 5218−5224.
15. Akiyama, Y., Shirai, Y., and Ito, K. (1994) *J. Biol. Chem. 269*, 5225−5229.
16. Broome-Smith, J. K., and Spratt, B. G. (1986) *Gene 268*, 341−349.
17. Edelman, A., Bowler, J. K., Broome-Smith, J. K., and Spratt, B. G. (1987) *Mol. Microbiol. 1*, 101−106.
18. Wang, R., O'Hara, E. B., Aldea, M., Bargmann, C. I., Gromley, H., and Kushner, S. R. (1998) *J. Bacteriol. 180*, 1929−1938.
19. Granger, L. L., O'Hara, E. B., Wang, R. F., Meffen, F. V., Armstrong, K., Yancy, S. D., Babitzke, P., and Kushner, S. R. (1998) *J. Bacteriol. 180*, 1920−1928.
20. Tomoyasu, T., Yamanaka, K., Murata, K., Suzaki, T., Bouloc, P., Kato, A., Niki, H., Hiraga, S., and Ogura, T. (1993) *J. Bacteriol. 175*, 1352−1357.
21. Akiyama, Y., Yoshihisa, T., and Ito, K. (1995) *J. Biol. Chem. 270*, 23485−23490.
22. Akiyama, Y., and Ito, K. (2001) *Biochem*istry *40*, 7687−7693.
23. Akiyama, Y., Kihara, A., Mori, H., and Ito, K. (1998) *J. Biol. Chem. 272*, 22326−22333.

24. Walker, J. E., Saraste, M., Runswick, M. J., and Gay, N. J. (1982) *EMBO J. 8*, 945−951.
25. Patel, S., and Latterich, M. (1998) *Trends Cell Biol. 8*, 65−71.
26. Vale, V. D. (2000) *J. Cell Biol. 150*, F13−F20.
27. Jiang, B. L., and Bond, J. S. (1992) *FEBS Lett. 312*, 110−114.
28. Lenzen, C. U., Steinmann, D., Whiteheart, S. W., and Weis, W. I. (1998) *Cell 94*, 525−536.
29. Shotland, Y., Koby, S., Teff, D., Mansur, N., Oren, D. A., Tatematsu, K., Tomoyasu, T., Kessel, M., Bukau, B., Ogura, T., and Oppenheim, A. B. (1997) *Mol. Microbiol. 24*, 1303−1310.
30. Karata, K., Verma, C. S., Wilkinson, A. J., and Ogura, T. (2001) *Mol. Microbiol. 39*, 890−903.
31. Jayasekera, M. M. K., Foltin, S. K., Olson, E. R., and Holler, T. P. (2000) *Arch. Biochem. Biophys. 380*, 103−107.
32. Burgess, R. R. (1996) *Methods Enzymol. 273*, 145−149.
33. Gentry, D. R., and Burgess, R. R. (1990) *Protein Expr. Purif. 1*, 81−86.
34. Liberek, K., Galitski, T., Zylicz, M., and Georgopoulos, C. (1992) *Proc. Natl. Acad. Sci. U.S.A. 89*, 3516−3520.
35. Kotlarz, A., Szalewska-Palasz, A., Wegrzyn, G., and Lipinska, B. (1998) *Biotechnol. Technol. 12*, 869−873.
36. Lanzetta, P. A., Alvarez, L. J., Reinach, P. S., and Candia, O. A. (1979) *Anal. Biochem. 100*, 95−97.
37. Hirst, T. R., Randall, L. L., and Hardy, J. S. (1984) *J. Bacteriol. 157*, 637−642.
38. Tadayyon, T. M., Gittins, J. R., Pratt, J. M., and Broome-Smith, J. K. (1994) *Membrane protein expression systems* (Gould, G. W., Ed.) p 64, Portland Press, London, UK.
39. Asahara, Y., Atsuta, K., Motohashi, K., Taguchi, H., Yohda, M., and Yoshida, M. (2000) *J. Biochem. 127*, 931−937.
40. Dean, F. B., Dodson, M., Echols, H., and Hurwitz, J. (1987) *Proc. Natl. Acad. Sci. U.S.A. 84*, 8981−8985.
41. Dean, F. B., and Hurwitz, J. (1991) *J. Biol. Chem. 266*, 5062−5071.
42. Bruckner, R. C., Crute, J. J., Dodson, M. S., and Lehman, I. R. (1991) *J. Biol. Chem. 266*, 2669−2674.

BI034516H